

Article

# Physical Properties of Plasma-Activated Water

Mobish Shaji <sup>1</sup>, Alexander Rabinovich <sup>1,\*</sup>, Mikaela Surace <sup>1</sup>, Christopher Sales <sup>2</sup> and Alexander Fridman <sup>1</sup><sup>1</sup> C and J Nyheim Plasma Institute, Drexel University, Camden, NJ 08103, USA<sup>2</sup> Department of Civil, Architectural and Environmental Engineering, Drexel University, Philadelphia, PA 19104, USA

\* Correspondence: ar483@drexel.edu

**Abstract:** Recent observations of plasma-activated water (PAW)'s surfactant behavior suggest that the activation of water with non-equilibrium plasma can decrease the surface tension of the water. This suggested change to the surface tension also indicates that the addition of plasma can lead to changes in the physical properties of the water, knowledge of which can expand existing PAW applications and open new ones. While the chemical behavior of PAW has been extensively analyzed, to the best of our knowledge the physical properties of PAW have not been investigated. This study focuses on the need for experimental determination of PAW's physical properties—namely, surface tension, viscosity, and contact angle. The experimental results of this study show that the addition of plasma lowers the surface tension of water at room temperature, increases the viscosity of water at high temperatures, and lowers the contact angle of droplets on glass surfaces at room temperatures. Potential factors influencing these changes include plasma alteration of the mesoscopic structure of water at low temperatures and plasma additives acting as foreign particles in water at higher temperatures. Ultimately, this investigation demonstrates that the physical properties of water change due to plasma activation, which could lead to potential industrial applications of PAW as a surfactant or as a washing-out and cleaning agent.

**Keywords:** plasma-activated water; PAW; physical properties; surface tension; viscosity; contact angle



**Citation:** Shaji, M.; Rabinovich, A.; Surace, M.; Sales, C.; Fridman, A. Physical Properties of Plasma-Activated Water. *Plasma* **2023**, *6*, 45–57. <https://doi.org/10.3390/plasma6010005>

Academic Editor:  
Andrey Starikovskiy

Received: 22 December 2022  
Revised: 13 January 2023  
Accepted: 18 January 2023  
Published: 30 January 2023



**Copyright:** © 2023 by the authors. Licensee MDPI, Basel, Switzerland. This article is an open access article distributed under the terms and conditions of the Creative Commons Attribution (CC BY) license (<https://creativecommons.org/licenses/by/4.0/>).

## 1. Introduction

Non-thermal plasmas generated in ambient air, as well as in oxygen- or nitrogen-containing working gases and noble gases, produce a variety of reactive oxygen and nitrogen species (RONS), e.g., ozone, hydroxyl radicals, hydrogen peroxide, superoxide, and nitrogen oxides. The interaction of plasma with liquid media leads to the transport of RONS into the liquid and the formation of secondary active species. In water, the main reactive species formed by plasma activation are OH radicals, ozone, hydrogen peroxide, nitrites, nitrates, peroxyxynitrites, and peroxyxynitrates; water activated in this way with non-thermal plasma is called plasma-activated water (PAW) [1]. PAW is considered to be a green and prospective solution for numerous biotechnology applications, due to the transient nature of its biochemical activity. The biochemical activity of PAW is derived from the synergistic effects of active species—especially RONS. PAW currently has numerous applications, including but not limited to surface disinfection, seed germination, use as a fertilizer, inactivation of plant-based pathogenic organisms, curing fungus-infected plants, food preservation, wound healing, deactivation of bacteria and viruses, mouthwash due to its bactericidal and fungicidal efficacy, selective killing of cancer cells, and insecticides [2–8].

Plasma-activated water, because of its active biological properties, has been extensively studied in order to understand plasma's interactions with water [9], the production and behavior of active species [1], differences in the production of active species under varying plasma gases [8], identification and quantification of chemical species [3], transfer of specific active species—namely, RONS species—to the liquid [10], and differences in the production of active species with varied plasma systems and production parameters [11]. As a result of these detailed

studies into the chemical behavior of PAW, there is an excellent understanding of PAW's chemical properties and biological behavior. For example, the antiviral behavior of PAW is attributed to the short-lived ONOO- species [5], the plant growth improvement effect of PAW is attributed to the aqueous nitrate, nitrite, and ammonium ions and hydrogen peroxide species [3], and the antibacterial properties of PAW are attributed to the short-lived reactive oxygen species [4]. Until this study, the investigated physicochemical properties of PAW included pH, ORP, and electrical conductivity; these properties were investigated in relation to the chemical properties and behavior of PAW, as they are indicators of reactive species in the PAW [12].

While scientific interest and the number of publications related to plasma control of the chemical properties of water are growing exponentially, to the best of our knowledge no studies to date have focused on the physical properties and physical behavior of PAW. In a recent study, J He et al. [13] observed that, while deactivating *E. coli* bacteria on the surface of fresh produce, PAW significantly washed out or physically removed the *E. coli* from the produce surface. While the RONS in PAW can deactivate bacteria, they cannot physically remove them. This bacterial washing-out behavior of PAW is an indicator of its low surface tension, or surfactancy. Therefore, these results suggest that the addition of plasma brings about changes in the thermodynamic properties (e.g., surface tension) of water. If the surface tension of the water is reduced via, plasma activation as suggested by J He et al. [13], the potential of PAW as a surfactant widens quickly, as there are numerous fields that could benefit from a liquid with anti-pathogenic and surfactant properties. Potential applications for PAW as a surfactant might include use as a washing-out and cleaning agent, an ingredient for eco-friendly detergents and soaps, surfactants for biomedical applications, and more. Furthermore, since we have an indication that the addition of plasma can change the surface tension of water, other physical properties of water could also be affected by the addition of plasma. Investigating these properties is important to finding areas of potential PAW applications.

Surface tension is the measure of force acting at the boundary of two phases. It refers to the elastic tendency of fluid surfaces that makes them acquire the least possible surface area. At the liquid–air interface, the greater attraction of liquid molecules to one another than to air molecules results in surface tension. Hence, the cohesive force between the liquid molecules is higher than the adhesive force between liquid and air molecules. This results in an inward force at the liquid surface that causes it to behave as if the surface were covered with an elastic membrane. Because of the high attraction of water molecules to one another, water has a high surface tension (0.0728 N/m at 20 °C) compared to many other liquids. The surface tension of a liquid can provide insights into its capillarity behavior, surfactant properties, etc. As a liquid with growing uses in the cleaning and agriculture industries, insights into the surface tension properties of PAW can be useful for its economical industrial adoption.

Viscosity, or more precisely shear viscosity, is the property that defines the quantitative relationship between the applied shear stress and the shear deformation rate in a fluid. Qualitatively, viscosity indicates the resistance to flow of a fluid. Since viscosity is the property that controls and quantifies the shear stress/shear rate behavior in fluids, it is in many regards the most important physical property of a fluid. Viscosity is stated in two different forms: the absolute or dynamic viscosity ( $\mu$ ), and the kinematic viscosity or momentum diffusivity ( $\nu$ ), where  $\nu = \mu/\rho$  and  $\rho$  is the fluid's density [14].

The contact angle is another fundamental property of interest when the interface between two fluids is also in contact with a surface, e.g., a water drop resting on a leaf. The contact angle is dependent on the surface energy of the solid and describes how liquids spread on a surface—vital information for dynamic liquid–solid processes such as coating and painting. In addition, precise measurements of the contact angle between a fluid–fluid interface and a solid surface are critical to deduce the wetting and spreading characteristics of liquids on surfaces, as well as to calculate the surface energy of a solid by measuring the contact angle of a series of liquids on one type of surface. These surface properties are important when considering, for example, the application of dyes to surfaces and pesticides to plants [15].

Since studies investigating the physical properties of PAW (such as surface tension, viscosity, and contact angle are very limited), there is a strong need to investigate these behaviors. Insights into the physical properties of PAW will provide users with a better understanding of the physical behavior of PAW and of plasma's interaction with water during PAW generation, and they will also help users identify properties that can be applied to present and future areas of need. In order to address this research gap, this study focuses on the changes occurring in the physical properties of water as a result of plasma activation—namely, the surface tension, viscosity, and contact angle of PAW.

## 2. Materials and Methods

### 2.1. PAW Production

The plasma-activated water used in this study was produced with gliding arc plasma. Gliding arc plasma is a transient non-equilibrium type of discharge with a relatively high microarc temperature (about 1600–1800 °K). In the gliding arc plasmatron (Figures 1 and 2), air is injected tangentially into the gap between two cylindrical electrodes, and a vortex of air is created in the gap. As energy is supplied between the high- and low-voltage electrodes, the plasma discharge occurs between the electrodes. The air vortex stretches and rotates the gliding arc, thereby producing the plasma zone inside the plasmatron. As water is injected into the plasmatron axially from the top, the water droplets react with the air that is coming out of the plasmatron, producing PAW. After being processed in the gliding arc plasmatron, different kinds of active species (such as OH radicals, hydrogen peroxide, NO<sub>x</sub>, etc.) are produced in the water. The pH of PAW is 2–2.9, as opposed to the 5.5–6 of distilled water. The operational parameters of the PAW production were as follows: 60–100 mL/min water flow rate; 40–100 SLPM plasma air flow rate. The experiment was performed using 400–1900 W plasma power. The gliding arc plasmatron used for PAW production in this study is shown in Figure 1, and a schematic of the gliding arc plasmatron's operational principle is shown in Figure 2.



Figure 1. Gliding arc plasmatron setup.

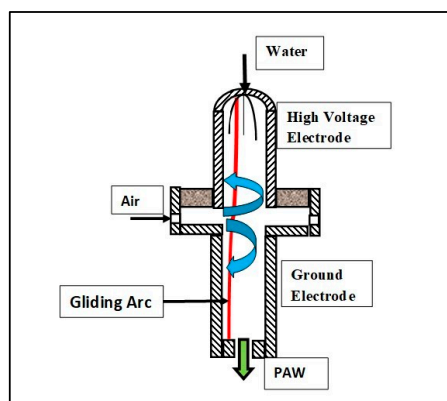


Figure 2. Working principle of the gliding arc plasmatron.

## 2.2. Surface Tension Measurement Method

For more than a century, a variety of techniques have been used to measure the interfacial tension between immiscible fluid phases. When we discuss the interfacial tension between a liquid and a gas, we call it surface tension. The different surface tension measurements are described in detail by Drelich et al. [16]. The different types of surface tension measurements can be divided into five groups: The first group of techniques directly measure the surface tension with a microbalance. Examples from this group include the Wilhelmy plate and Du Noüy ring methods. The second group of techniques determines surface tension through direct measurements of capillary pressure. Examples from this group include the maximum bubble pressure and growing drop methods. The third group of techniques relies on the balance between surface tension forces and variable volumes of liquid to determine the liquid's surface tension. Examples from this group include the capillary rise and drop volume methods. The fourth group of techniques is based on fixing the volume of the liquid and measuring the distortion of a drop of the liquid under the influence of gravity. Examples from this group include the pendant drop and sessile drop methods. The fifth group of techniques, used to measure ultralow surface tensions, involves distortion of the shape of the liquid using centrifugal force. The pendant drop method was chosen for surface tension measurements in this study, as it is the simplest, most robust, and most versatile method. Surface tension measurement using the pendant drop method consists of suspension of a liquid droplet from a needle [17].

Pendant drop tensiometry using OpenDrop software was chosen as the surface tension measurement method for this project because of its accuracy and open-source nature [16,17]. Pendant drop tensiometry is performed by generating droplets of the liquid to be analyzed using a syringe pump, capturing an image of the generated droplet, and iteratively fitting the Laplace equation on this droplet image using image-processing software to determine the surface tension of the liquid. Images of Pendant drop tensiometry performed are shown in Figures 3 and 4.



Figure 3. Image of a droplet during the pendant drop method.

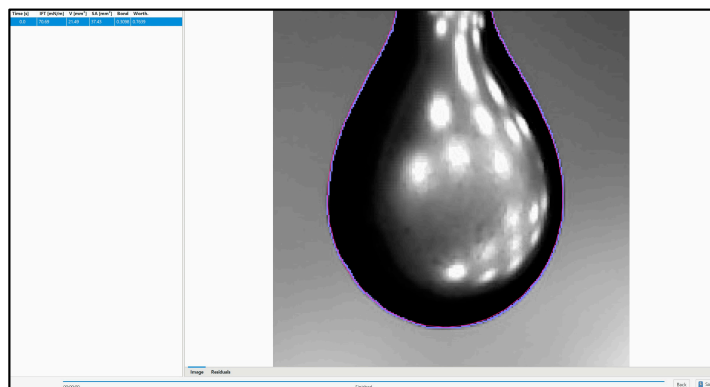


Figure 4. OpenDrop software fitting a Laplace equation over a droplet image.

The accuracy of this method was validated by correction factors with respect to image quality obtained from the image processing software, called Worthington and Bond numbers. The recommended numbers for accurate measurements are 0.7–0.8 for Worthington numbers and 0.3–0.35 for bond numbers [17]. The average Worthington and bond numbers for all measurements in this study were 0.77 and 0.31, respectively. The error in all instances was 0.01 for both Worthington and bond numbers. These measurements were taken at a room temperature of 18 °C.

### 2.3. Viscosity Measurement Method

Viscometers make use of the theoretical relationship between shear stress and strain rate to measure viscosity. There are three types of viscometer: flow, drag, and resonant. In flow-type viscometers, the rate of flow of the fluid in a tube or through an orifice is measured, and the shear stress can either be calculated or estimated based on theory. Examples of flow-type viscometers include capillary tube viscometers, with which shear stress is calculated, and cup viscometers, with which shear stress is estimated. Flow-type viscometers measure kinematic viscosity. Drag-type viscometers measure either the force on an object as it moves at a specified rate in the fluid (for example, rotational viscometers) or the time it takes for an object to move a specified distance through the fluid (for example, falling objects and bubble tube viscometers). Drag-type viscometers measure absolute viscosity. The third type of viscometer is the resonant or vibrational viscometer, which is most commonly used for in-line process applications [14].

Among the commercially available viscometers, a capillary viscometer was chosen for viscosity measurements in this study because it was cost-effective and readily available. Capillary viscometers determine viscosity by measuring the liquid flow rate through a capillary tube. These viscometers are typically made of glass and consist of a bulb reservoir connected to the capillary tube. The operation of a capillary tube viscometer is based on the Poiseuille model of laminar flow which, describes flow through a round pipe [14].

The capillary viscometer used for this study was a certified, calibrated, size 25 Cannon-Fenske viscometer. The certified accuracy of this device is 0.16%. The viscosity was measured from 10 to 40 °C with the help of a water bath. The setups of the viscometer and water bath are shown in Figures 5 and 6, respectively.



Figure 5. Cannon- Fenske viscometer.

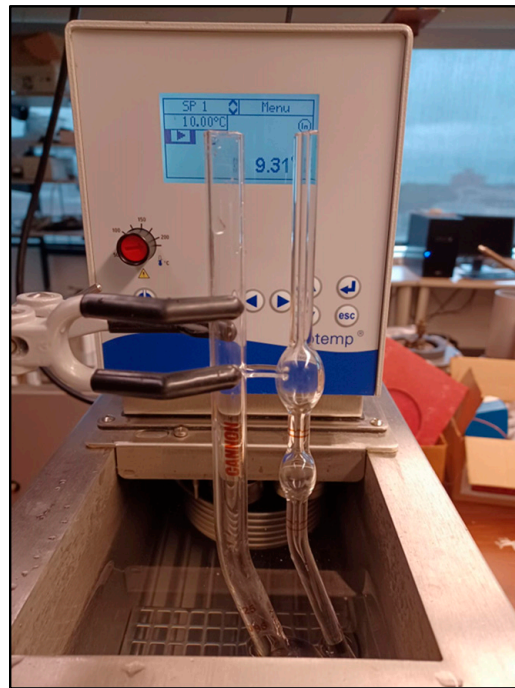


**Figure 6.** Viscosity measurement setup.

The Cannon-Fenske viscometer has two fluid reservoirs connected by a tilted capillary tube. A measured volume of the liquid to be analyzed is added to the lower reservoir. After equilibration at a constant temperature, the liquid is drawn up through the capillary tube to fill the second reservoir until it overfills. The liquid is then allowed to fall under the influence of gravity, and the time taken for the liquid meniscus to pass between two marks in the viscometer (as seen in Figure 5) is noted as the efflux time. The kinematic viscosity of the liquid, which is the mathematical product of the efflux time and certified viscosity constants, was calculated for each temperature point.

#### 2.4. Contact Angle Measurement Method

The most common contact angle measurement methods include the telescope–goniometer method, Wilhelmy balance method, captive bubble method, tilting plate method, and the more recently developed drop shape analysis methods. Among these methods, the most frequently used is direct measurement of the contact angle by telescope–goniometer. In this method, a direct measurement of the tangent angle is taken at the three-phase contact point on a sessile drop profile. Drop shape analysis of sessile drop also measures the tangent angle at the three-phase contact point with the help of droplet images and computer programs [18]. A simplified experimental setup of the drop shape analysis method suitable for researchers was used in this study for the measuring contact angle [19]. Droplets comprising 20  $\mu\text{L}$  of PAW and distilled water on clean glass microscope slides were captured as images, as shown below. The contact angle between the liquid droplets and the glass was measured using OpenDrop image processing software [17]. The contact angle made by 20  $\mu\text{L}$  of distilled water on a glass slide was measured to validate the accuracy of the measurement. The contact angle for distilled water determined by this method was  $54.5^\circ$ , which is consistent with the literature reports of  $\sim 55^\circ$  [20]. The images of the PAW droplet making a  $31^\circ$  contact angle on the glass surface and the distilled water droplet making a  $54.5^\circ$  contact angle on the glass surface are shown in Figures 7 and 8, respectively. The measurements were conducted at a room temperature of  $18^\circ\text{C}$ .

The surface tension and contact angle investigations in this study were limited to room temperature due to the limitations presented by the cost of systems required for accurately measuring these properties at varying temperatures.

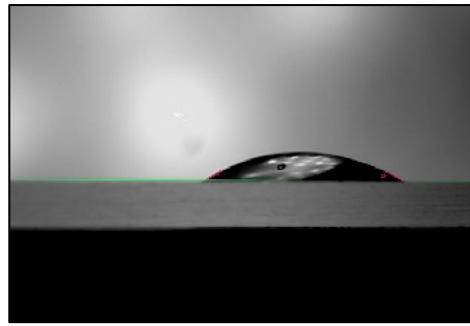


**Figure 7.** PAW droplet making a  $31^\circ$  contact angle on a glass surface.

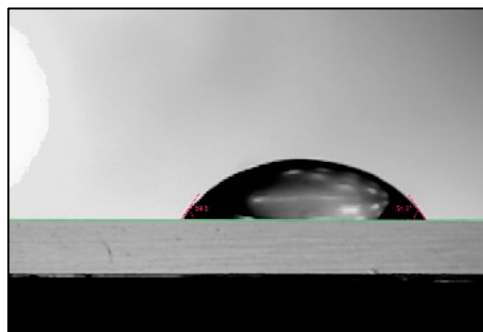


**Figure 8.** Distilled water droplet making a  $54.5^\circ$  contact angle on a glass surface.

### 3. Results

#### 3.1. Surface Tension of PAW

The surface tension of two PAW samples of pH 2.5 and pH 2.78 was measured using pendant drop tensiometry, at a room temperature of  $18^\circ\text{C}$ . The results obtained are shown in Figure 9. The literature values of water surface tension [21] is also included as a reference. The PAW at pH 2.5 had a surface tension of  $68.7\text{ mN/m}$ , while the PAW at pH 2.78 had a surface tension of  $68.6\text{ mN/m}$ —both lower than the surface tension of distilled water at  $18^\circ\text{C}$  reported in the literature, which was  $73.1\text{ mN/m}$ . On average, the PAW displayed a viscosity 6.1% lower than that of distilled water. The relative accuracy of the measurements was determined to be 3.65%.

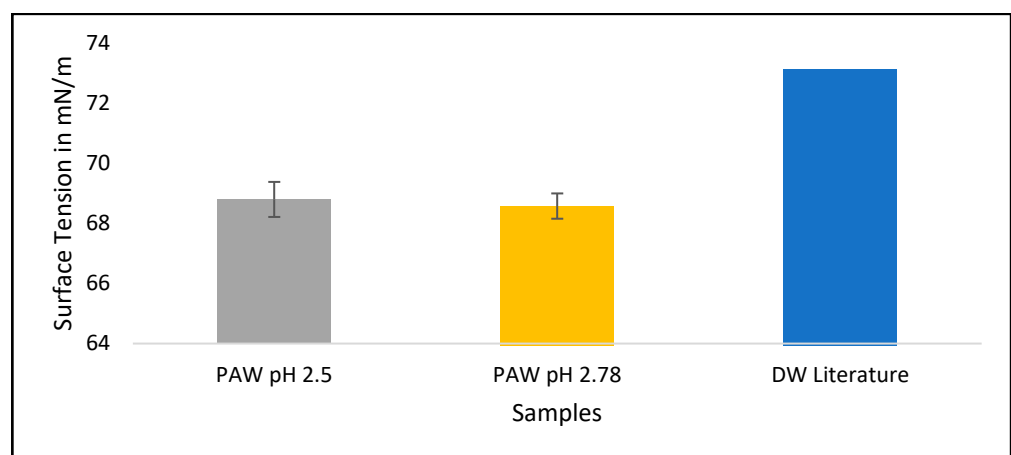


**Figure 9.** Surface tension of plasma-activated water at  $18^\circ\text{C}$ ; the surface tension of distilled water (DW) at this temperature is shown for reference.

Using the modified free energy equation, J He et al. [13] suggested that PAW's washing out (physical removal) of *E. coli* is aided by a reduction in the surface tension of water with the addition of plasma. The surface tension of water is lowered by the transition of

the crystalline mesoscopic structure of water to an amorphous mesoscopic structure with the addition of plasma. This transition in the water's structure is aided by the plasma lowering the mesoscopic transition temperature. The results of this study are consistent with the suggestion of J He et al. [13], showing that the addition of plasma lowers the surface tension of the water. As the addition of plasma changes the surface tension of water, it also influences its thermodynamic properties.

The mesoscopic structure of normal water is crystalline at temperatures below 35 °C, and it transitions to being amorphous at temperatures between 35 and 60 °C [13]. The crystalline structure is characterized by high surface tension and high viscosity, while the amorphous structure is characterized by lower surface tension and viscosity relative to the crystalline structure. One example of differences in the physical properties of water with different mesoscopic structures is that hot water is more effective in cleaning applications than cold water, due to the lower surface tension or surfactancy of hot water's amorphous structure compared to cold water's crystalline structure. As J He et al. [13] witnessed surfactant behavior/low surface tension in water at low temperatures, they suggested that the addition of plasma could possibly lower the temperature required for mesoscopic structural changes in water. The theoretical proof presented [13] in support of their claim is discussed later to enrich the understanding of PAW's physical behavior.

Reduction in surface tension increases the surfactant behavior exhibited by a liquid, making it more suitable for cleaning and removal of particles. Since plasma-activated water is biodegradable, it can be suitable for cleaning applications without harming the environment.

### 3.2. Viscosity of PAW

The mesoscopic structural changes and foreign plasma additives in PAW influence its viscosity. The structure change at low temperatures should reduce the viscosity of PAW, while the foreign plasma additive should increase its viscosity. The effect of foreign plasma additives in increasing the viscosity of water is similar to how sand added to water can affect its viscosity; foreign additives can lead to increased friction in the liquid flow, resulting in higher viscosities. Since it is proposed that the addition of plasma will result in mesoscopic structural changes in water at low temperatures, PAW should display lower to almost identical viscosity relative to water at low temperatures. This is because the viscosity-reducing effect of mesoscopic structural change at low temperatures can possibly be countered by the viscosity-increasing effect of foreign plasma additives. If the proposed mesoscopic structural change does not occur, PAW should have a higher viscosity at lower temperatures because of the foreign plasma additives. The foreign plasma additives should also cause PAW to have higher viscosity at higher temperatures. At temperatures above 35 °C, normal water has an amorphous structure [13], and the only influence differentiating the rheological behaviors of PAW and normal water is that of the plasma foreign additives.

The viscosity of PAW at pH 2.78 was measured from 10 to 40 °C using the Cannon-Fenske viscometer and water bath setup described earlier (as shown in Figure 6). The viscosity results obtained for this temperature range are shown in Figure 10. The kinematic viscosity of water from the literature is included for reference [22].

The kinematic viscosity of PAW at 10 °C was  $1.28 \text{ mm}^2/\text{s}$ , compared to the  $1.30 \text{ mm}^2/\text{s}$  kinematic viscosity of water at the same temperature. The viscosity of PAW was 1.3% lower than that of distilled water at 10 °C. The slightly lower viscosity of PAW at low temperatures supports the mesoscopic structural changes in water proposed by J He et al. [13]. Under normal conditions, PAW should have exhibited a higher viscosity, since the foreign plasma additives have the natural effect of increasing viscosity. The amorphous structure of PAW at low temperature might have countered the viscosity-increasing effect of the plasma additives, resulting in a lower viscosity than that of distilled water.

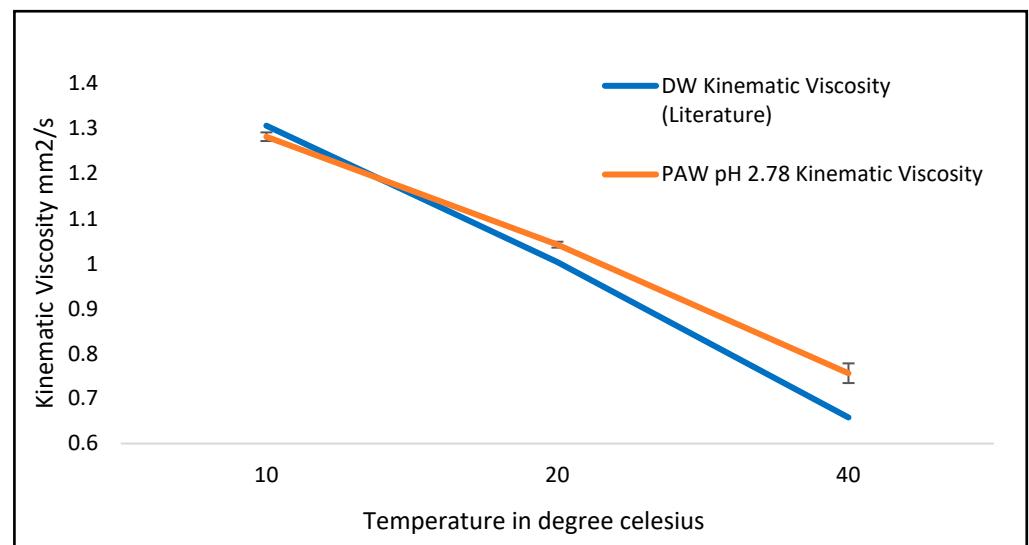


**Figure 10.** Viscosity of PAW from 10 to 40 °C; the viscosity of distilled water (DW) is shown for reference.

With the increase in temperature from 10 °C, the high viscosity of normal water, caused by its crystalline structure, started to decrease due to the transition of its structure to amorphous. As the crystalline structure in water began to weaken, the relatively lower viscosity of PAW, due to its amorphous structure, became less pronounced and began to match the viscosity of normal water, as demonstrated at about 15 °C in Figure 10.

With further increase in temperature from 15 °C, the higher viscosity of normal water due to its crystalline structure began to decrease as its structure transitioned further into amorphous, resulting in PAW having higher viscosity than normal water. The viscosity-reducing effect of the amorphous structure in PAW no longer countered the viscosity-increasing effect of its foreign plasma additives. The kinematic viscosity of PAW at 20 °C was 1.04 mm<sup>2</sup>/s, while that of normal water was 1.00 mm<sup>2</sup>/s; at 20 °C, the viscosity of PAW was 2.19% higher than that of normal water.

Following this trend of increased viscosity in PAW at higher temperatures, PAW at 40 °C had a kinematic viscosity of 0.76 mm<sup>2</sup>/s, while that of normal water was 0.66 mm<sup>2</sup>/s, meaning that PAW had a 12.8% higher viscosity than normal water at 40 °C. At 40 °C, the high viscosity caused by the crystalline structure was minimal in normal water, as its mesoscopic structure might have transitioned very close to amorphous; therefore, the higher viscosity demonstrated for PAW, which also has an amorphous structure, could be attributed to the foreign plasma additives.

### 3.3. Contact Angle of PAW

The difference in contact angles made by liquids on a surface helps us to understand the changes in surface energy between the liquids and the contacting surface. The contact angles made by PAW at pH values of 2.47, 2.68, and 2.85 on a glass microscope slide were inspected. The results obtained are summarized in Figure 11. The contact angle made by a distilled water droplet of the same volume in the same setup is shown for accuracy indication. The measurements were conducted at a room temperature of 18 °C.

PAW droplets make smaller contact angles on glass surfaces than water droplets, by an average of 20°, or 36%. At lower pH or higher plasma production power, PAW makes smaller contact angles. Therefore, the addition of plasma increases the surface energy during interaction between the glass surface and the water. The contact angle is an indication of the adhesive and cohesive forces exhibited by the liquid. If the adhesive force of a liquid is high relative to its cohesive force, the liquid will wet the surface more, resulting in a lower contact angle. If the cohesive force of the liquid is high relative to its adhesive force, the liquid will wet the surface less, resulting in a higher contact angle

formed on the surface. Since plasma activation resulted in water forming smaller contact angles, it increased the adhesive force of water during contact with glass. Therefore, plasma activation might increase the adhesive forces of liquids on surfaces; this could be useful in the surface treatment industry for applications requiring better adhesion by dyes, along with other applications that require better wettability of liquids to surfaces.

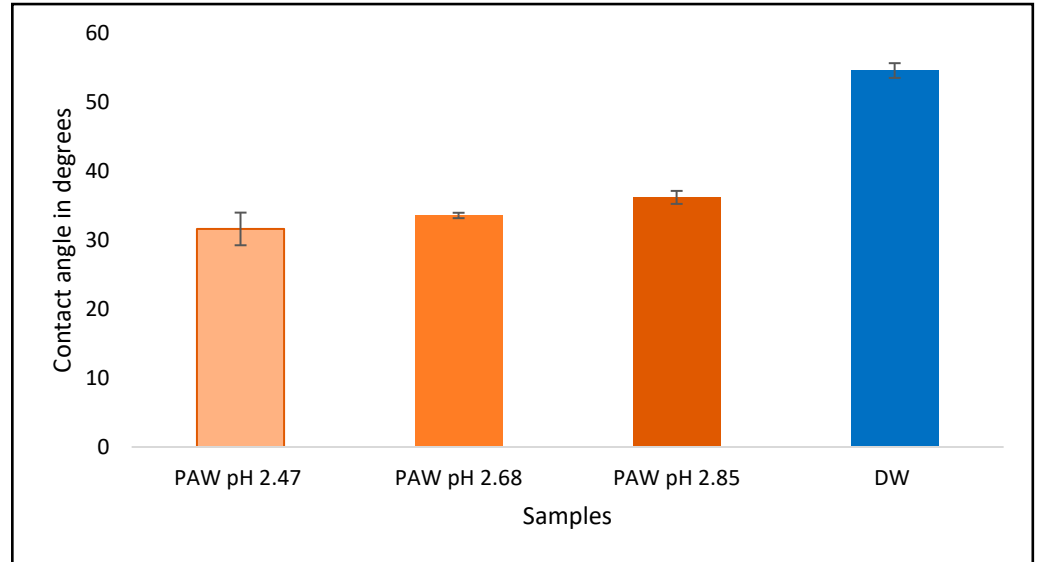


Figure 11. Contact angle made by PAW and distilled water (DW) on glass slides.

#### 4. Discussion

The low surface tension exhibited by water after plasma activation was attributed by J He et al. [13] to the plasma’s effect of lowering the mesoscopic transition temperature. The mesoscopic structure of water at lower temperatures is crystalline, which is characterized by higher surface tension and viscosity. However, as the temperature increases past the mesoscopic transition temperature, the crystalline structure of water changes to amorphous, which is characterized by lower surface tension and viscosity. J He et al. [13] suggested that plasma activation lowers the temperature required for this transition, causing PAW to display low surface tension and low viscosity at lower temperatures compared to normal water. J He et al. [13] theoretically demonstrated that plasma activation lowers the free energy of water. This can be shown with the following equation, where the free energy of water  $F$  is given by

$$\begin{aligned}
 F &= U - T \sigma + q (qV_s + (1 - q) V_r) \\
 &= qE_s + (1 - q)E_r + (qV_s + (1 - q)V_r)P \\
 &\quad + k_B T \left( q \ln \frac{q}{g_s} + (1 - q) \ln \frac{1-q}{g_r} \right)
 \end{aligned}
 \tag{1}$$

where  $F$  is the free energy of water,  $U$  is the internal energy of water,  $\sigma$  is the entropy,  $q$  is the percentage of structured state,  $E_{s,r}$  are the specific energies of the structured and random states, respectively ( $E_s < E_r$ ),  $V_{s,r}$  are the specific volumes,  $g_{s,r}$  are the statistical degeneracy values ( $g_s \ll g_r$ ),  $T$  is the temperature,  $P$  is the pressure, and  $k_B$  is the Boltzmann constant.

When ions are added to a fluid, it changes the fluid’s free energy. Free energy in the presence of ions contains an additional term, the Debye–Huckel term ( $U_{DH}$ ):

$$U_{DH} = - \sum_{i=1}^M \frac{N_i z_i^2}{2} \frac{e^2 \kappa}{4\pi \epsilon_r \epsilon_0} \frac{1}{1 + \kappa a_i}
 \tag{2}$$

$$\kappa^2 = \frac{2e^2}{\epsilon_r \epsilon_0 k_B T} \sum_{i=1}^M z_i^2 n_i
 \tag{3}$$

where  $i$  denotes the type of ion species,  $N_i$  is the ion's concentration,  $\alpha_i$  is the ion's radius,  $z_i$  is the charge of an ionic species,  $e$  is the charge of the electron,  $M$  is the total number of ionic species,  $\epsilon_r$  is the dielectric permittivity of the medium,  $\epsilon_0$  is the dielectric permittivity of a vacuum, and  $\kappa$  is the inverse of the Debye screening length. The ions are unlikely to penetrate the clusters; thus, in the first approximation, their impact is proportional to the percentage of water in the amorphous phase. From this, we can derive the free energy of plasma-activated water ( $F_{DH}$ ), modified with the Debye–Huckel term as follows:

$$F_{DH} = F + (1 - q)U_{DH} \quad (4)$$

From Equation (4), we can see that the addition of plasma 'favors' the amorphous state; thus, the transition temperature decreases.

PAW presents interesting behavior as a solution. An ideal solution is a solution whose properties change in proportion to the concentration of solute added to it. As PAW displays changes in properties (i.e., 6.1% for surface tension, 1.3–12.6% for viscosity, 36% for contact angle) that are significantly higher than the concentration of active species added to it (0.01%), we can conclude that PAW behaves non-ideally.

The low surface tension characteristic of PAW indicates potential surfactant behavior. Surfactants are required for numerous industrial processes, including but not limited to detergents, paints, food emulsions, biotechnological processes, biosciences, pharmaceuticals, and cosmetic products. PAW can be an eco-friendly and cost-effective alternative to current products used for these applications [23]. As PAW is antibacterial, antifungal, and has demonstrated its ability to disinfect bacteria [4] from fresh produce, it can be an excellent washing-out agent—an industrial process that prevents disease breakouts due to microbes on produce. Surfactants with antibacterial and antifungal properties are used in biomedical fields [23]; as PAW has these properties [4,7] and can act as a surfactant, it can potentially be applied as a biomedical industrial surfactant. Surfactants are also important ingredients for the preparation of detergents and cleaning agents. PAW with surfactant properties can potentially be used in these processes as a biodegradable and eco-friendly ingredient [23]. One major advantage of using PAW is its biodegradability [1], which means that it can meet the surfactant requirements for industrial processes without harming the environment.

The viscosity of PAW is influenced by the mesoscopic structural changes and the presence of foreign plasma additives due to plasma activation. At low temperatures, when the effect of the crystalline structure is dominant in water, PAW with its amorphous structure has a slightly lower viscosity. As temperatures increase beyond low values, the friction-inducing plasma additives result in higher viscosity in PAW when compared to water. Until the crystalline structure of water is transitioned to an amorphous structure, the viscosity of PAW is only nominally higher than the viscosity of water. However, as the temperature increases beyond the mesoscopic transition temperature in water (35° C [13]), and the water attains an amorphous structure, the friction-inducing plasma additives cause PAW to have a significantly higher viscosity than water (12.8%). The high viscosity of PAW can lead to higher shear force exerted by the liquid during its flow at high temperatures. The higher shear force exerted by the flow of PAW on a particle in its path can lead to better removal of particles when compared to normal water, making PAW a better cleaning agent at higher temperatures. The higher viscosity of PAW can also cause it to form a thicker boundary layer during flow, thereby reducing transfer losses and making it suitable for augmented oil extraction.

In terms of contact angle, the addition of plasma caused water to form smaller contact angles on a glass surface, indicating that the addition of plasma increases the surface energy during interaction between water and a glass surface. The addition of plasma resulted in increased wettability and increased adhesion of water to the glass surface. Increased wettability and adhesion are of great use for applications in the surface treatment industry. These improved surface properties exhibited by PAW suggest that plasma activation of liquids might result in improved adhesion and wettability by liquids thus activated, potentially improving the adhesive behavior of paints, dyes, etc.

## 5. Conclusions

The aim of this study was to experimentally investigate the understudied physical properties of PAW and see the effects of the addition of plasma to application-oriented physical properties—namely, surface tension, viscosity, and contact angle. This study inspected the surface tension and contact angle of PAW at room temperature (i.e., 18 °C) and the viscosity of PAW between 10 and 40 °C. The addition of plasma resulted in changes to the physical properties of water, as observed and theoretically suggested by J He et al. [13]. The major conclusions drawn from this study are as follows:

1. The physical properties of water change with plasma activation.
2. As a solution, PAW behaves non-ideally; since the percentage changes occurring to the physical properties with the addition of plasma are higher than the percentage of plasma species added.
3. The addition of plasma lowers the surface tension of water by 6.1% at room temperature; it also decreases the temperature required for the mesoscopic transition from crystalline to amorphous structure, resulting in lower surface tension in PAW relative to normal water.
4. The addition of plasma increases the viscosity of water by 12.8% at higher temperatures; foreign plasma additives lead to this increased viscosity in PAW. The viscosity-increasing effect of plasma additives is inhibited at low temperatures due to the PAW's amorphous structure.
5. The contact angle made by water on glass surfaces is reduced by 36% with plasma activation; thus, the surface energy during the interaction of water with glass is increased with plasma activation, thereby increasing the wettability and adhesion of water to the glass surface.
6. The changes occurring to the physical properties of water with plasma activation can be attributed to water attaining an amorphous structure at lower temperatures, as well as the presence of plasma additives at higher temperatures.

**Author Contributions:** Conceptualization, A.R., C.S. and A.F.; formal analysis, M.S. (Mobish Shaji) and M.S. (Mikaela Surace); investigation, M.S. (Mobish Shaji) and M.S. (Mikaela Surace); methodology, C.S.; project administration, A.R. and A.F.; supervision, A.R.; writing—original draft, M.S. (Mobish Shaji); writing—review and editing, A.R. and A.F. All authors have read and agreed to the published version of the manuscript.

**Funding:** This research received no external funding.

**Institutional Review Board Statement:** Not applicable.

**Data Availability Statement:** No new data were created or analyzed in this study. Data sharing is not applicable to this article.

**Conflicts of Interest:** The authors declare no conflict of interest.

## References

1. Zhou, R.; Zhou, R.; Wang, P.; Xian, Y.; Mai-Prochnow, A.; Lu, X.; Cullen, P.J.; Ostrikov, K.K.; Bazaka, K. Plasma-Activated Water: Generation, Origin of Reactive Species and Biological Applications. *J. Phys. Appl. Phys.* **2020**, *53*, 303001. [[CrossRef](#)]
2. Gapper, C.; Dolan, L. Control of Plant Development by Reactive Oxygen Species. *Plant Physiol.* **2006**, *141*, 341–345. [[CrossRef](#)] [[PubMed](#)]
3. Judée, F.; Simon, S.; Bailly, C.; Dufour, T. Plasma-Activation of Tap Water Using DBD for Agronomy Applications: Identification and Quantification of Long Lifetime Chemical Species and Production/Consumption Mechanisms. *Water Res.* **2018**, *133*, 47–59. [[CrossRef](#)] [[PubMed](#)]
4. Ma, R.; Wang, G.; Tian, Y.; Wang, K.; Zhang, J.; Fang, J. Non-Thermal Plasma-Activated Water Inactivation of Food-Borne Pathogen on Fresh Produce. *J. Hazard. Mater.* **2015**, *300*, 643–651. [[CrossRef](#)] [[PubMed](#)]
5. Guo, L.; Yao, Z.; Yang, L.; Zhang, H.; Qi, Y.; Gou, L.; Xi, W.; Liu, D.; Zhang, L.; Cheng, Y.; et al. Plasma-Activated Water: An Alternative Disinfectant for S Protein Inactivation to Prevent SARS-CoV-2 Infection. *Chem. Eng. J.* **2021**, *421*, 127742. [[CrossRef](#)] [[PubMed](#)]
6. Li, Y.; Pan, J.; Ye, G.; Zhang, Q.; Wang, J.; Zhang, J.; Fang, J. In Vitro Studies of the Antimicrobial Effect of Non-Thermal Plasma-Activated Water as a Novel Mouthwash. *Eur. J. Oral Sci.* **2017**, *125*, 463–470. [[CrossRef](#)] [[PubMed](#)]

7. Ten Bosch, L.; Köhler, R.; Ortmann, R.; Wieneke, S.; Viöl, W. Insecticidal Effects of Plasma Treated Water. *Int. J. Environ. Res. Public Health* **2017**, *14*, 1460. [[CrossRef](#)] [[PubMed](#)]
8. Rathore, V.; Nema, S.K. The Role of Different Plasma Forming Gases on Chemical Species Formed in Plasma Activated Water (PAW) and Their Effect on Its Properties. *Phys. Scr.* **2022**, *97*, 065003. [[CrossRef](#)]
9. Bruggeman, P.; Leys, C. Non-Thermal Plasmas in and in Contact with Liquids. *J. Phys. Appl. Phys.* **2009**, *42*, 053001. [[CrossRef](#)]
10. Kawasaki, T.; Koga, K.; Shiratani, M. Experimental Identification of the Reactive Oxygen Species Transported into a Liquid by Plasma Irradiation. *Jpn. J. Appl. Phys.* **2020**, *59*, 110502. [[CrossRef](#)]
11. Rathore, V.; Nema, S.K. A Comparative Study of Dielectric Barrier Discharge Plasma Device and Plasma Jet to Generate Plasma Activated Water and Post-Discharge Trapping of Reactive Species: Physics of Plasmas: Volume 29, No. 3. Available online: <https://aip.scitation.org/doi/10.1063/5.0078823> (accessed on 10 January 2023).
12. Rathore, V.; Patel, D.; Butani, S.; Nema, S.K. Investigation of Physicochemical Properties of Plasma Activated Water and Its Bactericidal Efficacy | SpringerLink. Available online: <https://link.springer.com/article/10.1007/s11090-021-10161-y> (accessed on 10 January 2023).
13. He, J.; Rabinovich, A.; Vainchtein, D.; Fridman, A.; Sales, C.; Shneider, M.N. Effects of Plasma on Physical Properties of Water: Nanocrystalline-to-Amorphous Phase Transition and Improving Produce Washing. *Plasma* **2022**, *5*, 462–469. [[CrossRef](#)]
14. Kutz, M. *Handbook of Measurement in Science and Engineering*; John Wiley & Sons: New York, NY, USA, 2016; Volume 3.
15. Huang, E.; Skoufis, A.; Denning, T.; Qi, J.; Dagastine, R.R.; Tabor, R.F.; Berry, J.D. OpenDrop: Open-Source Software for Pendant Drop Tensiometry & Contact Angle Measurements. *J. Open Source Softw.* **2021**, *6*, 2604.
16. Drelich, J.; Fang, C.; White, C.L. Measurement of Interfacial Tension in Fluid-Fluid Systems. *Encycl. Surf. Colloid Sci.* **2002**, *3*, 3158–3163.
17. Berry, J.D.; Neeson, M.J.; Dagastine, R.R.; Chan, D.Y.; Tabor, R.F. Measurement of Surface and Interfacial Tension Using Pendant Drop Tensiometry. *J. Colloid Interface Sci.* **2015**, *454*, 226–237. [[CrossRef](#)] [[PubMed](#)]
18. Yuan, Y.; Lee, T.R. Contact Angle and Wetting Properties. In *Surface Science Techniques*; Springer: Berlin/Heidelberg, Germany, 2013; pp. 3–34.
19. Lamour, G.; Hamraoui, A.; Buvailo, A.; Xing, Y.; Keuleyan, S.; Prakash, V.; Eftekhari-Bafrooei, A.; Borguet, E. Contact Angle Measurements Using a Simplified Experimental Setup. *J. Chem. Educ.* **2010**, *87*, 1403–1407. [[CrossRef](#)]
20. Mohsin, H.; Sultan, U.; Joya, Y.F.; Ahmed, S.; Awan, M.S.; Arshad, S.N. Development and Characterization of Cobalt Based Nanostructured Super Hydrophobic Coating. *IOP Conf. Ser. Mater. Sci. Eng.* **2016**, *146*, 012038. [[CrossRef](#)]
21. Vargaftik, N.B.; Volkov, B.N.; Voljak, L.D. International Tables of the Surface Tension of Water. *J. Phys. Chem. Ref. Data* **1983**, *12*, 817–820. [[CrossRef](#)]
22. Huber, M.L.; Perkins, R.A.; Laesecke, A.; Friend, D.G.; Sengers, J.V.; Assael, M.J.; Metaxa, I.N.; Vogel, E.; Mareš, R.; Miyagawa, K. New International Formulation for the Viscosity of H<sub>2</sub>O. *J. Phys. Chem. Ref. Data* **2009**, *38*, 101–125. [[CrossRef](#)]
23. Fatma, I.; Sharma, V.; Kumar, A. Application of Surfactants for Better Tomorrow. *J. Phys. Conf. Ser.* **2022**, *2267*, 012125. [[CrossRef](#)]

**Disclaimer/Publisher's Note:** The statements, opinions and data contained in all publications are solely those of the individual author(s) and contributor(s) and not of MDPI and/or the editor(s). MDPI and/or the editor(s) disclaim responsibility for any injury to people or property resulting from any ideas, methods, instructions or products referred to in the content.